RESEARCH ARTICLE

Editorial Process: Submission:02/27/2024 Acceptance:07/12/2024

Comparative Analysis of the Apparent Diffusion Coefficient and Diffusion Tensor Imaging in the Diagnosis of Prostate Cancer

Kanat Karakoishin[1,2]*, Zhamilya Zholdybay[1], Akmaral Ainakulova[1], Yulduzkhan Dauytova[1], Vitaly Kamhen[3]

Abstract

Objective: The aim of this work was to demonstrate capabilities of diffusion tensor imaging as a diagnostic tool for prostate cancer in comparison with the apparent diffusion coefficient. **Methods:** 364 patients with suspected prostate cancer underwent multiparametric magnetic resonance imaging including diffusion tensor imaging. **Results:** The anatomical structure of the prostate obtained on T2-weighted imaging was compared with the apparent diffusion coefficient and diffusion tensor imaging maps. The rest of the gland (central and peripheral regions) were used as healthy areas. The apparent diffusion coefficient at diffusion-weighted imaging, fractional anisotropy and mean diffusivity at diffusion tensor imaging were evaluated in pathological zones. Cancer-suspicious areas of the prostate had high fractional anisotropy fractional anisotropy and low mean diffusivity compared to unaltered areas. Fractional anisotropy values were significantly elevated in central gland cancer, compared to normal tissue, and slightly elevated in peripheral zone cancer. **Conclusion:** Diffusion tensor imaging has the potential to identify prostate cancer with high accuracy and specificity. The combination of standard magnetic resonance imaging and diffusion tensor imaging can significantly improve the prognosis of the disease during active surveillance. The fractional anisotropy and mean diffusivity values can be useful in assessing the grade of malignancy and the radiolopathological correlation of the lesion.

Keywords: Mean diffusivity- multiparametric magnetic resonance imaging- diffusion- weighted imaging

Asian Pac J Cancer Prev, **25 (7)**, 2397-2408

Introduction

Prostate cancer is among top diseases in the world in terms of high incidence and mortality worldwide. Acute problem of early diagnosis of prostate cancer is connected not only with the late treatment of patients, but also with the insufficient accuracy of traditional diagnostic methods. The complexity of visualization of tumor foci in the prostate gland remains an urgent task, despite the modern development of methods for imaging the prostate gland. Despite the large number of screening programs, transrectal ultrasound (TRUS) guided prostate biopsy remains an essential diagnostic step that assists in final diagnosis or clarifies the prevalence of the process in the prostate. Systematic TRUS-guided biopsy is effective in diagnosing prostate cancer, but due to lack of targeting for a specific lesion, it often leads to overdiagnosis of clinically insignificant (ciPC) and underdiagnosis of clinically significant prostate cancer (csPC) [1]. Thus, the search for new methods of diagnosing prostate cancer that reduce the need for repeated biopsies remains relevant [2].

Multiparametric magnetic resonance imaging (mpMRI) shows sufficient sensitivity and specificity in the evaluation of prostate cancer [3, 4]. However, recent study by Stabile et al. [2] suggests that mpMRI is ineffective in detecting cancer with a Gleason score (GS) of ≤7 [5-8]. One of the elements of multiparametric magnetic resonance imaging (MRI) is diffusion-weighted imaging (DWI) [3,9], which is successfully used in the detection and localization of clinically significant prostate cancer [10]. DWI is based on the multidirectional thermal shifting of water molecules in tissue structures that may be isotropic (homogeneous and uniform in all directions) and anisotropic, in which, depending on the type, components and architectonics of tissues that are a physiological barrier, the movement of water molecules is inhomogeneous in one direction or another [11]. A recent study with 124 consecutive men with suspected prostate carcinoma underwent MRI and DWI; results demonstrated a substantial decrease in acquisition time while maintaining comparable prostate carcinoma evaluation rate and increasing global image quality [12]. Diffusion tensor imaging (DTI), in turn, takes into account the dependence of the movement of water

*[1]Department of Visual Diagnostics, Asfendiyarov Kazakh National Medical University, Almaty, Republic of Kazakhstan. [2]Department of Radiology, Medical Center "Sunkar", Almaty, Republic of Kazakhstan. [3]Department of Health Policy and Organization, Al-Farabi Kazakh National University, Almaty, Republic of Kazakhstan. *For Correspondence: k.karakoishin@hotmail.com*

molecules in tissues on direction. Fractional anisotropy (FA) and mean diffusivity (MD) are the indexes obtained using a DTI that provide information about changes in tissue microstructure, as shown by a recent study [13]. Moreover, authors suggest innovative quantitative indexes obtained from DTI and DTI tractography such as fiber tract density therefore support the application of DTI in the evaluation of advanced prostate carcinomas. Thus, in another study, prostate biopsy was performed based on mpMRI, ultrasound data, using systematic and targeted biopsy [14].

No scientific papers were aimed to highlight the importance of mentioned parameters in characterizing prostate cancer. Tractography DTI rebuilds fiber bundles in three dimensions, allowing visual assessment of tissue microstructures. Some papers have shown extensive periprostatic plexus within prostate tissue in patients with carcinomas using DTI tractography [13, 14]. Tractography offers unique insights into the microstructural environment and anatomical disruptions induced by prostate tumors by reconstructing and visualizing the 3D paths of fiber bundles. Mapping the periprostatic nerve plexus, a densely innervated network encircling the prostate gland, is one important use. Maintaining sexual and urinary function following prostate cancer treatment depends on protecting this nerve supply. Tractography patterns of malignant and non-cancerous prostates can be compared to identify indications of tumor-induced neuronal invasion or relocation. Additionally, by monitoring deviations from or displacements of typical anatomical fiber pathways, tractography has demonstrated potential for evaluating patterns of seminal vesicle invasion and extracapsular extension. Decisions about therapy could be made using this knowledge to enhance local staging. Still, it remains uncertain whether DTI prostate fiber tractography can ensure in vivo any data confirming or consistent with an increase in nerve fiber density within the prostate cancer tissue itself, which requires further research.

The application of DTI was assessed by DTI quantitative indexes and compared with conventional indexes. The correlation of DTI outcomes with Gleason grade was assessed. The Gleason grading system is a tool for assessing the aggressiveness and prognosis of prostate cancer. It grades the cancer from 1 (most well-differentiated) to 5 (most poorly differentiated) based on its histological patterns. The Gleason score, which ranges from 2 (1+1) to 10 (5+5), is calculated by summing the two most common pattern grades. Greater tumor aggressiveness, a higher risk of metastasis, and worse patient outcomes are all indicated by higher GS. However, there is a lack of information and comparative analyses about measured diffusion coefficient and diffusion tensor imaging in the diagnosis of prostate cancer. Consequently, the aim of this research is to undertake a comparative analysis of measured diffusion coefficient and diffusion tensor imaging in the diagnosis of prostate cancer. The study was based on the following tasks. First, a theoretical analysis was performed on the application of diffusion tensor imaging for diagnosis of prostate carcinomas. Secondly, a comparative analysis of the measured diffusion coefficient and diffusion tensor imaging in the diagnosis of prostate cancer was carried out. Finally, a comparative analysis of available similar works, including the results of this study, was carried out.

Theoretical Overview

Among oncological diseases in men in a number of countries, prostate cancer ranks second after lung carcinomas, and in the USA, it ranks first. According to the World Cancer Research Fund International's latest data [15], some of the countries with the highest age-standardized incidence rates of prostate cancer per 100,000 men include: Guadeloupe (France), Martinique (France), Ireland, Barbados, Saint Luvia, Estonia, Puerto Rico, Sweden, France and Bahamas. Recently is seen an exceptionally rapid increase in the incidence of prostate carcinomas, reaching an average of 3% incidences. According to the results of autopsy and prostatectomy, there is a significant frequency of clinically undiagnosed pathological changes in the prostate gland. Clinically undetectable malignant degeneration of the prostate gland occurs in 30.7% of men over 70 years of age [16]. Until recently, "small" prostate cancer was considered clinically insignificant, as it rarely has infiltrative growth. New data show that the course of the disease in small tumors is almost unpredictable and depends mainly on their biological activity [17, 18].

Diagnosis of prostate cancer at the primary stage has acquired particular relevance in recent years due to the emergence of real opportunities for radical surgical treatment. However, despite the rapid development of MRI possibilities the diagnosis of "low grade" cancer presents certain clinical difficulties [19]. Most diagnostic programs are based on a combination of three basic methods. These include palpation of the prostate gland through the rectum, blood serum analyses for prostate-specific antigen (PSA) and also TRUS followed by histological verification. Prostatic carcinomas are manifested by local tissue compaction. For this reason, palpation is relatively subjective and depends on the experience of the doctor [20]. Small-sized tumors, topographically located near the anterior surface and in the middle part of the gland are also not available for examination. PSA is an organ-specific marker that is overexpressed in case of malignant growth or even inflammatory processes, benign hyperplasia that makes it a reliable and sensitive predictor tool [21, 22].

Nowadays diagnosis of prostate cancer is using ultrasound methods due to the implementation of new advanced ultrasound techniques, including transrectal prostatic elastography, contrast-enhanced ultrasound, as well as improved B-mode, micro-ultrasound and micro-Doppler techniques. Many authors combine these methods under the general name of multiparametric ultrasound (mpUS) [22]. Recent studies indicate a high sensitivity of mpUS, similar to mpMRI [23]. Micro-ultrasound provides a clearer visualization of suspicious areas of the prostate [24]. The presence of cancer is indicated by a higher elastic modulus, asymmetric distribution on elastography, enhancement with a non-uniform distribution of the suspicious area on contrast-enhanced ultrasound [23]. However, these methods are not highly accurate when applied separately. The revealed changes are not strictly

specific for prostate cancer. Areas of a similar nature can be seen in acute prostatitis and in benign prostatic hyperplasia. The combination of these methods cannot fully replace mpMRI, and is only considered as an addition to mpMRI [25].

TRUS-guided biopsy is the basic method for diagnosing prostatic malignant neoplasms in patients with elevated PSA [26] that often leads to complications [27]. The presence of cancer signs on MRI is indicated by lower signal intensity on T2-weighted (T2WI), restriction on diffusion-weighted images, early enhancement on dynamic contrast sequences (DCE), and a higher ratio of choline on spectroscopic images [28-30]. In addition, some suspicious lesions may be localized in areas of the prostate that are difficult to visualize and may be missed on MRI [31]. One of the elements of MRI widely used in medical practice is DWI that allows a quantitative analysis of tissue microstructure by measuring the apparent diffusion coefficient (ADC). Diffusion tensor imaging allows quantitative analysis of anisotropic diffusion by plotting diffusion vectors and measuring diffusion along these vectors [12]. Diagnosis of prostate diseases is based on the data of digital rectal examination (DRE), evaluation of PSA levels, TRUS and MRI. Generally, diagnostic protocols for patients with prostate cancer are based on a combination of three methods – PSA, DRE and TRUS. Morphological confirmation of the diagnosis is provided by biopsy [20].

Still there is no common view on the use of imaging techniques for evaluation of primary prostate cancer. It is recommended that the choice of imaging technique should depend on specific questions to be answered for each individual patient. The development and implementation of an algorithm for conducting an MRI investigation using spectroscopy, DWI, and DTI, followed by a quantitative assessment of the data obtained for the differential diagnosis of benign and malignant prostate tumors, is an important issue for clinical research.

Materials and Methods

The issue of diagnosing prostate cancer is very social, but its importance is not fully understood by society. Currently, there is no single effective method for diagnosing prostate cancer (PCa). Existing methods are used at different stages – primary or clarifying diagnosis. The research protocol was created in the background of the Sunkar Diagnostic and Treatment Center data in Almaty, Kazakhstan. 364 patients with suspected prostate cancer aged median [IQR] 65.5 [60-71.75] were included in the study. Inclusion criteria for the study were men with suspected prostate cancer and elevated PSA levels as well as signed informed consent. Exclusion criteria included contraindications for MRI and inability to make a decision and/or sign an informed consent form. The standard mpMRI protocol was supplemented with the DTI protocol. mpMRI was performed on a 3T scanner (SignaArchitect, GE) using a surface coil. The data collection was represented by the following steps:

1. Axial T2-weighted turbospin echo with fast relaxation T2WI frFSE(TR/TE 4249/102.7 ms, cut thickness 4 mm, 0.5 mm gap, matrix dimensions 352×288 mm, rotation angle (FLIP) 111, number of averages (NEX) 1, scan time 2:52 min).

2. Sagittal T2-weighted sequence of turbospin echo with periodically rotated overlapping parallel lines with improved reconstruction T2WI Propeller (TR/TE 10490/86.0 ms, cut thickness 4 mm, 0.4 mm gap, matrix 320×320 mm, rotation angle (FLIP) 160, number of averages (NEX) 2.05, scan time 5:53 min).

3. Axial T1-weighted turbospin echo sequence with fat suppression T1WI FSE FS(TR/TE 751/9.2 ms, slice thickness 4 mm, with 0.5 mm gap, 384×224 mm matrix, rotation angle (FLIP)111, number of averages (NEX)1, scan time 3:59 min).

4. Coronal T2-weighted turbospin echo sequence with fast relaxation T2WI frFSE(TR/TE 5253/102 ms, cut thickness 4 mm, 0.5 mm gap, martiz 412×320 mm, rotation angle (FLIP) 160, number of averages (NEX) 2, scan time 4:55 min).

5. Coronal T1-weighted turbospin echo sequence T2WI FSE(TR/TE 693/8.5 ms, cut thickness 4 mm, 0.5 mm gap, matrix 320×320 mm, rotation angle (FLIP) 111, number of averages (NEX) 0.5, scan time 1:55 min).

6. Diffusion-weighted DWI with echo-planar series (TR/TE 5400/75.3 ms, slice thickness 4 mm with 0.5 mm gap, matrix 120×120 mm, three b-values (50, 600, 1000 s/mm^2), angle of rotation (FLIP) 90, number of averages (NEX) 2, scanning time 3:57 min).

To plot the DTI, 28 direction of the diffusion gradient was used; echo duration TE – 91.2 ms; repeating time TR – 5396 ms; cut thickness 3 mm without gaps between slices; field of view FOV – 200×209 mm; matrix dimensions – 128×80; voxel size – 1.56×2.6 mm^2, rotation angle FLIP – 90; b-values – 0 and 600 s/mm^2, number of averages (NEX) – 1, scan time 4:27 min.

The b-value of 600 s/mm^2 is a relatively low value. Better signal-to-noise ratios and reduced susceptibility to perfusion effects are typically associated with lower b-values, which can be helpful for prostate imaging. The 28 diffusion gradient directions selected were the result of balancing acquisition time and angular resolution. Higher angular resolution and improved diffusion anisotropy characterization can be achieved with more diffusion gradient directions; however, this comes at the cost of longer scan times. The authors used 28 directions in an attempt to strike a fair balance between these variables, allowing for a 4.3-minute scan time that was still enough for gathering diffusion tensor information.

The anatomical structure of the prostate obtained on T2WI was compared with the ADC and the DTI maps. The images were acquired in multiple planes (axial, sagittal, and coronal). The central gland (comprising the central and transitional zones) and peripheral zone of the prostate gland were delineated. Regions of interest (ROIs) were manually marked, corresponding to cancer-suspicious areas in those zones. The rest of the prostate and peripheral region of the prostate were used as healthy areas. Using the VolumeViewer software on a workstation (GE), the apparent diffusion coefficient ADC at DWI, fractional anisotropy FA and general diffusivity MD at DTI were evaluated in the region of interest. Prostate biopsy was

performed based on mpMRI, ultrasound data, using systematic and targeted biopsy.

For statistical evaluation of obtained data Microsoft Excel and the IBM SPSS Statistics package were used; T-test was used to evaluate differences in scores, DWI ADC, DTI metrics between normal indexes and malformed neoplasms. Authors used combined data on diagnostic test results and data on biopsy-confirmed PCa, as well as the results of association statistics: Fisher's Exact Test and odds ratio. The Fisher's Exact Test determines the significance of the relationship between two categorical variables, in this example, the presence or absence of biopsy-confirmed prostate cancer and the findings of the DTI/DWI test (positive or negative). Fisher's Exact Test results showing a statistically significant association ($p \leq 0.05$) between the DTI/DWI metric and prostate cancer status suggest that the metric has discriminatory potential. The odds ratio, which shows the likelihood of a positive test result in cancer patients relative to those without cancer, measures the strength of this link. When a test result is positive, the probability of having prostate cancer is higher when the odds ratio is larger than 1, and it is lower when the odds ratio is less than 1. Authors calculated sensitivity and specificity by comparing them with the results obtained from standard Prostate Imaging Reporting and Data System (PI-RADS) v2.1 mpMRI assessments. Additional analyses of obtained data were carried out by the means of receiver operating characteristic (ROC) curve analyses and area under the curve (AUC).

Results

Scientific research was aimed to perform MRI using the DTI detection method in 52 patients that have been included in studies and have signed informed agreement. The mean patient among investigated ages was 65.5 years (by inter-quartile range: 60-71.75). The mean index of PSA serum marker was 9.5 points (obtained by the inter-quartile range: 6.3-9.8 ng/mL). The mean prostate volume index was found to be 47.5 points (obtained by inter-quartile range: 26.75-53.75). Table 1 presents the general characteristics of the patient cohort investigated in this study.

All investigated patients were admitted to ultrasound-guided biopsy procedures of the prostate gland in the framework of conducted scientific research. Prostate cancer of different histological types and localization was diagnosed by the means of above mentioned clinical diagnostic methods in totally eight studied patients. Table 2 breaks down the distribution of GSs among the 56 patients diagnosed with prostate cancer. Among detected patients, totally 28 had a GS 7 of prostate cancer and 14 patients have shown a Gleason count 8 of prostate cancer. Only 7 patients had a Gleason count, 6 patients had prostate cancer, and 7 patients had a GS 9.

Table 3 summarizes the topographical localization of the prostate cancer lesions within the gland for the 56 patients diagnosed with PCa. This table emphasizes how crucial it is to take into account the precise location of prostate cancer lesions, since the anatomical region may have an impact on possible disease development, treatment plans, and methods for diagnosis.

The Gleason grading system is one of the most significant prognostic variables for prostate cancer. Prostate cancerous areas typically have higher FA values than prostate tissue in general, most likely as a result of cellular density alterations and microstructure disarray. Higher Gleason grade tumors have a more noticeable increase in FA. Lower MD values are typically correlated with higher GSs in DTI-derived MD, which indicates the more compact and cellular character of aggressive tumors. Grading prostate cancer has found that one of the most useful criteria is the ADC produced from DWI. It has been shown that there is a significant negative link between the GS and ADC, with higher Gleason grades being associated with lower ADC values. This is explained by the fact that more aggressive tumors have more cells and less extracellular space, which limits the transport of water.

When analyzing quantitative measurements of DTI and DWI in detected malignant lesions, MD showed low values in central part of gland (both transitional zone and central zone of the prostate gland) cancer $(535 \pm 125.33) \times 10^{-6}$ mm^2/s ($p=0.0011$) (mean±SD); and in cancer lesion of the peripheral zone within the prostatic tissue $(549.62 \pm 162.64) \times 10^{-6}$ mm^2/s ($p=0.0154$), if compared to normal tissue without neoplasma. FA values were significantly elevated in the central part gland of the prostate gland (transitional zone and central zone of the prostate gland) cancer $(0.4208 \pm 0.1467) \times 10^{-6}$ mm^2/s ($p<0.0001$) (mean±SD), if compared to normal tissue. Also it was slightly elevated in the peripheral zone of prostatic cancer $(0.381 \pm 0.145) \times 10^{-6}$ mm^2/s ($p<0.0001$) (Table 4). DTI:FA PCa was found to be $(0.4208 \pm 0.1467) \times 10^{-6}$ mm^2/s ($p<0.0001$) with the mean difference that equals 0.207 which is twofold higher if compared to the normal parameter of (0.214±0.0704) in case of central glans malignant process.

Table 5 presents a totally combined data on the diagnostic tests results and data on biopsy-confirmed PCa, as well as the results of association statistics: Fisher's Exact Test and odds ratio. The analysis revealed a statistically significant relationship/dependence between the diagnostic ability of the DWI:ADC tests (central and peripheral areas of the gland), DTI:FA (central and peripheral areas of the gland) and DTI:MD (peripheral area) tests to correctly determine the presence of PCa in patients. The Fisher's Exact Test statistic is significant at the $p \leq 0.01$ level. The diagnostic ability of the DTI:MD (central gland) PCa test was not statistically confirmed: the significance of Fisher's Exact Test was $p=0.108$. Authors obtained the results indicating that diagnostic DTI:FA values (peripheral zone) greater than 0.25 increase the chance of clinical verification of PCa by 70 times, DWI:ADC values (central gland) less than 700-37 times, DWI:ADC values (peripheral zone) less 700-30 times, DTI:FA values (central gland) more than 0.250-18.667 times and DTI:MD values (peripheral zone) less than 600-13 times.

Table 6 presents the sensitivity and specificity data of the provided diagnostic tests for prostate cancer patients. It was found that the highest sensitivity value

Table 1. General Characteristics of Investigated Patients

	All (n=364)	No cancer (n=308)	PCa (n=56)	Significance score
Age, median [IQR]	65.5 [60-71.75]	65.2 [58.25-71]	67.3 [63-72]	p=0.19
PSA in serum (ng/mL), median [IQR]	9.5 [6.3-9.8]	8.1 [6.2-9.5]	17.2 [8-17.5]	p=0.08
Prostate tissue size measured with MRI (mL), median [IQR]	47.5 [26.75-53.75]	46.1 [25.25-61]	55.6 [37.75-53.75]	p=0.23

(87.5%) is typical for such diagnostic tests as DWI:ADC combination (central gland), DTI:FA (central gland) and also DTI:FA (peripheral zone). It has also shown a significantly lower value for DTI:MD (central gland and peripheral zone) – 62.5% and DWI:ADC (peripheral zone) – 75%. The highest specificity value (90.9%) was observed in such tests as DWI:ADC (peripheral zone) and DTI:FA (peripheral zone), and a lower value for DTI:MD (peripheral zone) – 88.6%, DWI:ADC (central gland) – 84.1%, DTI:FA (central gland) – 72.7% and DTI:MD (central gland) – 70.5% in observed patients. For the peripheral zone the highest indexes were found to be within DTI:FA diagnostic test usage (sensitivity level 0.875). For the central zone the highest indexes were found to be within DWI:ADC diagnostic test usage (sensitivity level 0.875) and DTI:FA (sensitivity level 0.875). Specificity levels were found to be much more diverse if compared to sensitivity levels.

Along with the determination of sensitivity and specificity values, plots of sensitivity versus specificity were plotted. Figure 1 shows the ROC-curves of the diagnostic ability of the logistic regression model for PCa verification. The constructed curves for the DTI:FA and DWI:ADC tests used to diagnose the central gland of the DTI:FA, DWI:ADC and DTI:MD tests used to diagnose peripheral zones with respect to biopsy-verified PCa occupy a position in the upper left corner of the graph to a greater extent, which indicates acceptable diagnostic properties of tests. The curve of the DTI:MD test for diagnosing the central gland is located relatively closer to the reference line, which allows to make an assumption about the lower diagnostic properties of this conducted test.

At the final stage, the area under the ROC curves was also estimated (Table 7). According to the results obtained from the area under the ROC curves, the highest diagnostic accuracy is characteristic of the DTI:FA test used to diagnose the peripheral zone prostate cancer (area 0.933) that emphasizes its practical diagnostic value in management of patients with malignant processes. In second place is the DWI:ADC test (peripheral zone of the prostate gland) with the general evaluated area of 0.909, in third place it is the DTI:MD conducted test (peripheral zone of the prostate gland) with an area of 0.896, in fourth place is the DTI:FA test (central gland) with an area of 0.895, in fifth place is the DWI:ADC test (peripheral zone) with an area of 0.889 and in sixth place is the DTI:MD test (central gland) with an area of 0.787. The first five tests are

Table 2. Gleason Score Indexes in Patients Diagnosed with Prostate Cancer

Score	n (%)
Gleason 6 (3+3)	8 (12.5)
Gleason 7 (3+4)	28 (50)
Gleason 7 (4+3)	-
Gleason 8 (4+4)	14 (25)
Gleason 9 (4+5)	7 (12.5)

Table 3. Localization of the Lesion in Prostate Gland in Studied Patients

Topographical localization of the tumor	n (%)
Peripheral zone of gland	21 (37.5)
Central part of the gland	28 (50)
Central part of the gland and the peripheral zone	7 (12.5)

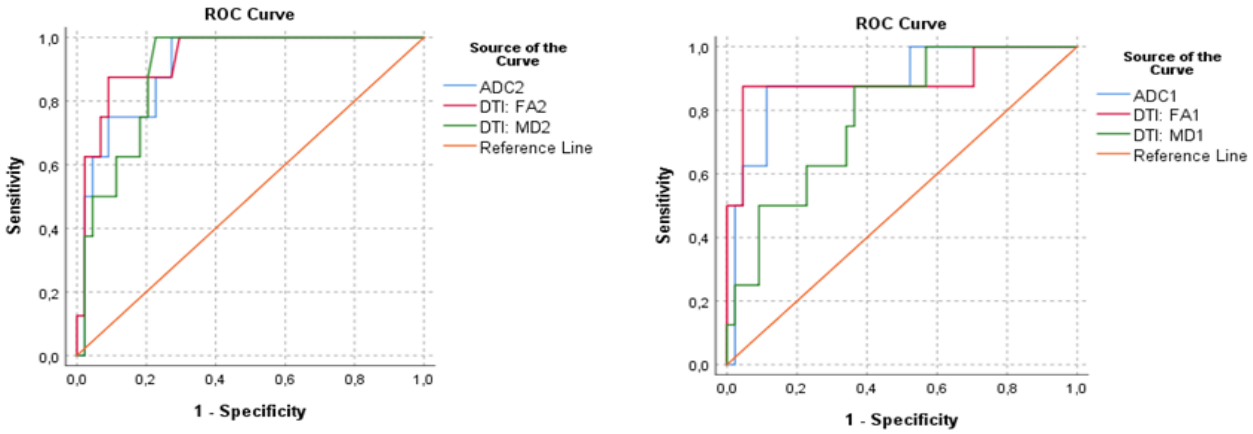

Figure 1. ROC-Curves of Diagnostic Possibilities of the Logistic Lapsing Model of PCa Verification: a) Central gland; b) Peripheral zone

Table 4. DTI and DWI Indexes in Normal and Malignant Neoplasms of the Prostate Gland, for (a) the peripheral region; and (b) the central region (transitional and central areas) in studied patients

Evaluated parameter	Normal index (10^{-6} mm^2/s)	PCa (10^{-6} mm^2/s)	Mean Difference (10^{-6} mm^2/s)	Significance score
(a) Peripheral Zone				
DTI:FA	0.143±0.091	0.381±0.145	0.239	<0.0001
DTI:MD	992.73±367.78	535±125.33	-457.73	0.0011
DWI:ADC	1279.66±457.91	651.12±228.71	-628.53	0.0004
(b) Central Gland				
DTI:FA	0.214±0.0704	0.4208±0.1467	0.207	<0.0001
DTI:MD	767.04±233.99	549.62±162.64	-217.421	0.0154
DWI:ADC	885.25±173.93	610.12±157.24	610.12	0.0001

Table 5. Baseline Test Results and Data on Biopsy-Confirmed PCa and Association Statistics

Diagnostic tests	PCa		Fisher 's Exact Test Statistics	Odds ratio
	There is	No		
DWI:ADC (central gland)				
Less than 700	49	49	Fisher's Exact Test=0.00018, P<0.001	37
More than 700	7	259		
DWI:ADC (peripheral zone)				
Less than 700	42	28	Fisher's Exact Test=0.00025, P<0.001	30
More than 700	14	280		
DTI:FA(central gland)				
More than 0.250	49	84	Fisher's Exact Test=0.00231, P=0.002	18.667
Less than or equal to 0.250	7	224		
DTI:FA(peripheral zone)				
More than 0.250	49	28	Fisher's Exact Test=0.00002, P<0.001	70
Less than or equal to 0.250	7	280		
DTI:MD (central gland)				
Less than 600	35	91	Fisher's Exact Test=0.10759, P=0.108	3.974
The probability of verification is low	21	217		
DTI:MD (peripheral zone)				
Less than 600	35	35	Fisher's Exact Test=0.00409, P=0.004	13
The probability of verification is low	21	273		

characterized by a high (an excellent) quality of predictive clinical accuracy. Additionally, the DTI:MD test (central and transient zone of the prostate gland) has an average level of predictive accuracy. This data should be concerned when an individual diagnostic tactic is admitted.

The gold standard for imaging in the diagnosis and characterization of prostate cancer is now mpMRI. It integrates several functional magnetic resonance imaging (fMRI) techniques, including magnetic resonance spectroscopy (MRS) and dynamic contrast-enhanced MRI (DCE-MRI). During a gadolinium-based contrast agent injection, serial MRI images are acquired prior to, during, and following the procedure known as DCE-MRI. DCE-MRI can identify regions of suspicious enhancement

Table 6. Sensitivity and Specificity of Conducted Diagnostic Tests for Patients with Prostate Cancer of Different Localization and Histological Type

Diagnostic tests	Sensitivity level	Specificity level
DWI:ADC (central gland)	0.875	0.841
DWI:ADC (peripheral zone)	0.75	0.909
DTI:FA(central gland)	0.875	0.727
DTI:FA (peripheral zone)	0.875	0.909
DTI:MD (central gland)	0.625	0.705
DTI:MD (peripheral zone)	0.625	0.886

Table 7. Area under the Curve and Obtained Asymptotic Significance

Diagnostic tests	Area [DE]	Asymptotic significance
DWI:ADC (central part of gland)	0.889 [0.733/1]	p=0.001
DWI:ADC (peripheral zone)	0.909 [0.820/0.998]	p<0.001
DTI:FA(central gland)	0.895 [0.733/1]	p<0.001
DTI:FA(peripheral zone)	0.933 [0.856/1]	p<0.001
DTI:MD (central gland)	0.787 [0.635/0.939]	p=0.01
DTI:MD (peripheral zone)	0.896 [0.808/0.985]	p<0.001

that can be indicative of clinically significant tumors by examining the contrast kinetic curves. MRS is an effective technique that can identify raised levels of specific metabolites, such as a higher ratio of choline+creatine/citrate, that are linked to prostate cancer. These variations in metabolism within the prostate gland can be mapped spatially by MRS using single- or multi-voxel spectroscopic techniques. High spatial resolution, full non-invasiveness, and lack of exogenous contrast agents are the advantages of DTI and DWI over DCE-MRI and MRS. Because prostate tumors have high cellular densities that limit water transport, DWI in particular provides a high sensitivity for detecting prostate malignancies. DTI offers more details regarding the directionality of water transport, which is helpful in determining the aggressiveness and microstructure of tumors.

As part of an extensive mpMRI strategy for the evaluation of prostate cancer, DTI and DWI are frequently paired with T2-weighted anatomical imaging and frequently DCE-MRI in contemporary clinical practice. The complementary data from several methods improves the accuracy of the diagnosis. Despite MRS's high level of specificity, its availability and lengthier scan periods prevent it from being used everywhere. Prostate cancer identification and characterization will probably benefit greatly from the distinct information that DTI and DWI measures offer, especially as quantitative modelling and machine learning techniques to synthesize mpMRI data advance.

Discussion

The rapid development of medical technologies in recent decades has led to the sharp emergence of highly informative methods, the use of which has already become an essential part of everyday medical practice and cancer patients management. However, there remains a stable tendency for misinterpretation of prostate diseases, including false positive or false negative results, which affects the further management of patients and their quality of life. To date, the study of prostate cancer using multiparametric MRI with subsequent classification of changes using the PI-RADS is the essential approach in the evaluation and detection of prostate carcinomas that is used worldwide.

Given the visualizing possibilities of 3T MRI, parallel imaging technologies, and ultrafast single echo-planar sequences, DWI and DTI have become more applicable to examining the abdominal and pelvic organs, including the prostate gland. 3T MRI provides a sufficient increase in the signal-to-noise index, higher spatial and temporal quality and reduces the time of image acquisition. The main disadvantage of 3T is the increase in sensitivity artefacts during procedure. However, the use of the parallel imaging technique, by reducing the number of acquired sensitivity artefacts, provides much informative data in the outcome.

This paper was aimed to assess DTI using Fisher's Exact Test, odds ratio, and quantification of diffusion rates. All scales showed good detection accuracy for PCa, with peripheral zone AUC calculated from quantification reaching 0.93 (95% CI 0.85-1) for FA values derived from DTI compared to 0.9 (95% CI 0.82-0.99) for ADC indexes received from DWI. The central and transient zone AUC reached 0.89 (95% CI 0.73-1) for FA indexes, obtained from DTI, in compression with 0.88 (95% CI 0.73-1) for ADC values derived from DWI. Peripheral, central and transient zone AUCs for MD, derived from DTI, showed slightly reduced values of 0.89 (95% CI 0.8-0.98) and 0.78 (95% CI 0.63-0.93) respectively, compared with ADCs derived from DWIs of 0.90 (95% CI 0.82-0.99) and 0.88 (95% CI 0.73-1). These obtained results are close to previous scientific findings [32]. As mentioned by authors of the current study, minimum tumor MD and the ratio of minimum tumor in studied patients show the same highest correlation with Gleason score and DTI method. Between GS $\leq$7 and GS $\geq$7, variations are statistically valuable for evaluated MD indexes but for some fractional anisotropy evaluations. MD performs better measurements than FA in discriminating GS$\geq$7(4+3). Overall, such tools can be implemented in assessing peripheral zone prostate carcinomas grade and patient's prognosis.

In this study, a 28-direction diffusion gradient was applied, which allowed to reduce the scanning time to 4.3 min, which differs slightly from previously published works [33-36]. Like most researchers, the authors of the current study used the DTI software on a workstation to measure ROI MD and FA [37-42]. Some other researchers in their studies used additional software to measure diffusion coefficients, which showed very good results in the diagnosis of prostate cancer [36,43]. However, these softwares are not available for all MRI devices, and require additional qualifications of the radiologist, which makes their use difficult in the routine examination of patients with suspected prostate cancer.

The results of MD derived from DTI, like previous studies, showed lower values in PCa compared to normal tissue [44, 45], results of FA derived from DTI showed higher values in PCa compared to normal tissue, which agrees with the results of some studies [37, 43, 45], but disagrees with the outcomes of papers, where values were either of the same level [46] or even lower [47]. Some researchers claim that DTI has better negative and positive evaluational indexes than mpMRI to track prostate cancer in target groups of patients (obtained positive predictive value (over 75%) [36]. One may assume that DTI combined with T2-weighted imaging may possess the potential to ameliorate prostate cancer identification without mandatory contrast injection or invasive procedures [44]. These assumptions do correlate with obtained data.

Proposed conducted work is a prospective study that has compared DTI, ADC, PI-RADS2, with more efficient use of a standard protocol for cancer patients and workstation software for DTI analysis. Work used a b-value of 0 and 600 s/mm^2 to obtain the DTI, which is comparable to some studies [40, 44], however in some studies the b-value was below 600 s/mm^2 [42, 46, 48] or above 600 s/mm^2 [38, 41, 47]. More specifically, some other researchers demonstrate that the microscopic component of T2-weighted imaging and the practical feature of DTI should be used in a combination to more

successfully evaluate the development of prostate tumor extensions [45]. The current study demonstrates the high efficiency of DTI with a low b-value and a relatively small amount of diffusion gradient direction in the diagnosis of prostate cancer. Scientists claim that fractional anisotropy shows high positive correlation with prostate cancer GS as well as median diffusivity negative correlation with GS [35]. Eventually, combined quantitative parameter indexes and DTI maps can be more actively implemented to conduct assessment of prostate cancer course and overall survival prognosis, helping in the improvement of the management protocol of cancer patients, that relates to the outcomes of conducted research. Additional approval to obtained results comes from study that shows the use of the b-value range and b-value that improve the contrast and discriminative power of DTI while evaluating prostate cancer [46]. The sensitivity of DTI indexes to age-related microstructural histological changes is statistically valuable. FA and MD may show microstructural changes associated with ageing of the prostate, such as vascular remodeling and changes in tissue architecture. Consequently, these implies that DTI indexes may be sensitive biomarkers for evaluating how ageing affects prostate microstructure [49, 50].

DWI has also shown to be an effective method for prognostication and therapy response prediction. The predictive relevance of DWI-derived ADC values in immunocompetent patients with primary central nervous system lymphoma (PCNSL) was examined by Mulyadi et al. [51]. The researchers discovered, through a number of investigations, that lower pretreatment ADC was associated with poorer clinical outcomes, such as a shorter progression-free and overall survival period in PCNSL patients. Thus, DWI appears to have potential as a low-cost, non-invasive imaging biomarker for risk-stratifying these patients before starting treatment. This would make it possible to use more individualized treatment plans based on the DWI measurements' prediction of cancer aggressiveness. In addition to its prognostic value, diffusion-weighted MRI has also demonstrated efficacy in evaluating tumor aggressiveness and proliferative activity. EL Sayed et al. [52] explored the role of DWI in assessing the aggressiveness of rectal cancers and correlating with the Ki-67 proliferation marker. The researchers discovered that more aggressive tumor features, such as lymphovascular invasion and perineural invasion, were substantially correlated with lower ADC values on preoperative DWI. Beyond simple detection, DWI is becoming increasingly useful in therapeutic settings for a variety of cancer types.

Metabolomics, the comprehensive study of small molecule metabolites in biological systems, has emerged as a promising tool for cancer diagnostics, including prostate cancer. Lamasz et al. [53] highlighted that metabolomics can provide insights into the distinct metabolic profiles associated with malignant transformation and tumor progression. Metabolomics provides a means of identifying cancer-specific metabolic patterns that could be used as diagnostic biomarkers by analyzing biofluids such as blood, urine, or tissue samples. Metabolomic investigations in the context of prostate cancer have revealed differences in the amounts of metabolites, including sarcosine, citrate, and different lipids, between patients with malignancies and healthy controls. The dysregulated metabolic pathways causing unchecked cancer cell growth and proliferation are reflected in these metabolic alterations. As analytical techniques and data analysis methodologies continue to progress, metabolomics presents itself as a highly specific, less intrusive strategy for early prostate cancer detection and diagnosis that may be used in conjunction with other screening tools such as PSA testing and radiologic imaging.

Hirna et al. [54] investigated how patients with oral and oropharyngeal malignancies responded to chemotherapy and radiation therapy by looking at the immunomodulating effects of alpha/beta-defensin preparations. The investigators emphasized the possible modulation of the body's response to cytotoxic treatments using adjuvant therapy. Similar strategies combining immunomodulators and chemotherapy/radiation therapy may be studied in the future for prostate cancer to increase anti-tumor effects and enhance diagnostic precision by changing metabolic profiles that can be identified by imaging or liquid biopsy analyses, or by improving tumor visibility. Combination tactics like these could offer a more complete picture of how the cancer behaves and responds to therapy. In an Asian cancer center, Yuin et al. [55] investigated the clinical results of stereotactic body radiation therapy (SBRT) for localized illness. Studies such as these strengthen the data base supporting radiation treatments in the management of prostate cancer, even if the main focus was on treatment efficacy and toxicity. When combined with sophisticated imaging techniques for target definition and post-treatment response evaluation, radiation may help to characterize and diagnose diseases. For example, following SBRT, alterations in quantitative imaging may assist distinguish treatment-induced residual disease from residual disease.

Kozłowski et al. [56] examined the occurrence and clinical characteristics of hepatocellular carcinoma (HCC) in the north-eastern region of Poland. The researchers emphasized the value of imaging studies and alpha-fetoprotein (AFP) screening in the identification and treatment of HCC. Given that high levels of the tumor marker AFP can suggest the existence of HCC, it is frequently utilized in the screening and monitoring of the condition. Because they provide precise visual information about the size, location, and spread of the tumor, imaging techniques like MRI and computed tomography (CT) are essential for the diagnosis and staging of HCC. The researchers stressed that the diagnostic workup and clinical assessment of patients with suspected or confirmed HCC require the concurrent use of AFP screening and imaging modalities such as CT and MRI.

Trifonov et al. [57] in their study describe the synthesis and evaluation of novel 7-aza-coumarin-3-carboxamide compounds for anticancer activity. Because these unique chemicals can specifically target cancer cells while preserving healthy tissues, they show promise as diagnostic agents. They are good candidates for use in imaging procedures like positron emission tomography

(PET) or MRI due to their distinct chemical structure and particular interactions with cancer cell receptors or biomarkers. Clinicians may be able to see prostate tumors with greater specificity and sensitivity by combining these chemicals with imaging agents, which would allow for more precise disease staging and diagnosis. Moreover, these substances may be employed in conjunction with current diagnostic instruments to augment their effectiveness or function as supplementary agents in multimodal imaging methodologies.

It is recommended to use DTI in addition to standard mpMRI in clinical protocols for prostate cancer patients because it can have high predictive value in PI-RADS 3 lesions when the probability of prostate cancer is yet unclear. The DTI can be used in selecting areas of the prostate for targeted biopsy investigation, as well as in separating patients into those who require systematic biopsy and those who do not. Such results will lead to a more qualified and effective management of cancer patients on the primary stages of its diagnostics and verification.

In conclusions, the noted results allow to conclude that DTI with the calculation of the MD and FA in the diagnosis of prostate cancer is expedient. The statistical analysis presented in the article and experimental research data proved the efficacy of the implementation of diffusion tensor tomography in the diagnosis of prostate cancer and the complete correspondence of visual informativeness data and statistical parameters to the prognostic value of MRI studies. Therefore, the effectiveness of diffusion tensor tomography in the diagnosis of prostate cancer is high, which is explained by the advantages of structural and spatial resolution, as well as the specific processing of the information received and a rigorous research algorithm.

Cancer-suspicious areas of the prostate had high fractional anisotropy FA and low mean diffusivity MD compared to unaltered areas were as follows: MD showed low values in central gland cancer (535±125.33)×10-6 mm^2/s ($p=0.0011$) (mean±SD) and in cancer in peripheral zone (549.62±162.64)×10-6 mm^2/s ($p=0.0154$), compared to normal tissue; FA values were significantly elevated in central gland cancer (0.4208±0.1467)×10-6 mm^2/s ($p<0.0001$) (mean±SD), compared to normal tissue, and slightly elevated in peripheral zone cancer (0.381±0.145)×10-6 mm^2/s ($p<0.0001$). DWI:ADC of the central gland, DTI:FA of the central gland and DTI:FA of the peripheral zone showed higher sensitivity values (87.5%) than DTI:MD of the central and peripheral areas – 62.5% and DWI:ADC in peripheral zone – 75%. DTI has the potential to identify prostate cancer with high accuracy and specificity. In addition, this preliminary study proves the feasibility of measuring prostate DTI, proposing that specialized software evaluation of DTI scores combined with DWI and T2-weighted visualization could ameliorate PCa diagnosis without usage of contrast methods.

Although the study's results are encouraging, there are a number of significant limitations that need to be taken into account. The retrospective nature of the analysis and the 364 patients from a single center in the sample size are two possible sources of bias. More extensive, prospective multi-center studies with uniform inclusion and exclusion standards are required to confirm and enhance the applicability of these results. The inability to directly compare this method of prostate cancer detection to other well-established imaging techniques is another drawback. It is necessary to conduct future head-to-head studies evaluating the diagnostic performance of DTI/DWI against other sophisticated imaging modalities in the same patient groups. There is an inherent constraint in relying just on MRI-guided and systematic biopsy data to determine the ground truth cancer status because sampling mistakes may have missed certain clinically relevant malignancies. Ideally, specimens from radical prostatectomy with thorough histological mapping might be included in subsequent validation to conclusively verify the existence and degree of illness. This would allow for detailed tumor localization/grading and imaging measures to be correlated voxel-wise.

Additional validation research is recommended to verify the outcomes of this and other similar experimental studies. More research on the influence of DTI and DTI tractography on diagnostic and predicting factors is needed to confirm preliminary data.

Author Contribution Statement

All authors contributed to the study conception and design. Material preparation, data collection and analysis were performed by Kanat Karakoishin, Zhamilya Zholdybay and Akmaral Ainakulova. The first draft of the manuscript was written by Yulduzkhan Dauytova and Vitaly Kamhen and all authors commented on previous versions of the manuscript. All authors read and approved the final manuscript.

Acknowledgements

General

None.

Ethical Declaration

All procedures performed in studies involving human participants were in accordance with the ethical standards of the institutional and national research committee and with the 1964 Helsinki declaration and its later amendments or comparable ethical standards. A study was approved by National Ethics Commission of the Asfendiyarov Kazakh National Medical University October 21, 2023, No 1043-B.

Data Availability

The data that support the findings of this study are available on request from the corresponding author.

Study Registration

The study was registered at the Sunkar Diagnostic and Treatment Center data in Almaty, Kazakhstan.

Conflict of Interest

The authors declare no conflict of interest.

References

1. Richenberg J, Løgager V, Panebianco V, Rouviere O, Villeirs G, Schoots IG. The primacy of multiparametric MRI in men with suspected prostate cancer. Eur Radiol. 2019;29(12):6940-52. https://doi.org/10.1007%2Fs00330-019-06166-z.
2. Stabile A, Giganti F, Rosenkrantz AB, Taneja SS, Villeirs G, Gill IS, et al. Multiparametric MRI for prostate cancer diagnosis: Current status and future directions. Nat Rev Urol. 2020;17(1):41-61. https://doi.org/10.1038/s41585-019-0212-4.
3. Hamoen EHJ, de Rooij M, Witjes JA, Baranetz JO, Rovers MM. Use of the prostate imaging reporting and data system (PI-RADS) for prostate cancer detection with multiparametric magnetic resonance imaging: A diagnostic meta-analysis. Eur Urol. 2015;67(6):1112-21. https://doi.org/10.1016/j.eururo.2014.10.033.
4. Fütterer JJ, Briganti A, De Visschere P, Emberton M, Giannarini G, Kirkham A, et al. Can clinically significant prostate cancer be detected with multiparametric magnetic resonance imaging? A systematic review of the literature. Eur Urol. 2015;68(6):1045-53. https://doi.org/10.1016/j.eururo.2015.01.013.
5. Bratan F, Niaf E, Melodelima C, Chesnais AL, Souchon R, Mège-Lechevallier F, et al. Influence of imaging and histological factors on prostate cancer detection and localisation on multiparametric MRI: A prospective study. Eur Radiol. 2013;23(7):2019-29. https://doi.org/10.1007/s00330-013-2795-0.
6. Selnæs KM, Heerschap A, Jensen LR, Tessem MB, Schweder G, Goa P, et al. Peripheral zone prostate cancer localization by multiparametric magnetic resonance at 3 T: Unbiased cancer identification by matching to histopathology. Invest Radiol. 2012;47(11):624-33. https://doi.org/10.1097/RLI.0b013e318263f0fd.
7. Turkbey B, Mani H, Shah V, Rastinehad AR, Bernardo M, Pohida T, et al. Multiparametric 3T prostate magnetic resonance imaging to detect cancer: Histopathological correlation using prostatectomy specimens processed in customized magnetic resonance imaging based molds. J Urol. 2011;186(5):1818-24. https://doi.org/10.1016/j.juro.2011.07.013.
8. Le JD, Tan N, Shkolyar E, Lu DY, Kwan L, Marks LS, et al. Multifocality and prostate cancer detection by multiparametric magnetic resonance imaging: Correlation with whole-mount histopathology. Eur Urol. 2015;67(3):569-76. https://doi.org/10.1016/j.eururo.2014.08.079.
9. Weinreb JC, Barentsz JO, Choyke PL, Cornud F, Haider MA, Macura KJ, et al. PI-RADS Prostate imaging – Reporting and data system: 2015, version 2. Eur Urol. 2016;69(1):16-40. https://doi.org/10.1016/j.eururo.2015.08.052.
10. Tamada T, Kido A, Yamamoto A, Takeuchi M, Miyaji Y, Moriya T, et al. Comparison of biparametric and multiparametric MRI for clinically significant prostate cancer detection with PI-RADS version 2.1. J Magn Reson Imaging. 2021;53:283-91. https://doi.org/10.1002/jmri.27283.
11. Ranzenberger LR, Das JM, Snyder T. Diffusion tensor imaging. Treasure Island: StatPearls Publishing; 2023.
12. Jendoubi S, Wagner M, Montagne S, Ezziane M, Mespoulet J, Comperat E, et al. MRI for prostate cancer: Can computed high b-value DWI replace native acquisitions?. Eur Radiol. 2019;29(10):5197-204. https://doi.org/10.1007/s00330-019-06085-z.
13. Gholizadeh N, Greer PB, Simpson J, Denham J, Lau P, Dowling J, et al. Characterization of prostate cancer using diffusion tensor imaging: A new perspective. Eur J Radiol. 2019;110:112-20. https://doi.org/10.1016/j.ejrad.2018.11.026.
14. Panebianco V, Barchetti F, Sciarra A, Marcantonio A, Zini C, Salciccia S, et al. In vivo 3D neuroanatomical evaluation of periprostatic nerve plexus with 3T-MR Diffusion Tensor Imaging. Eur J Radiol. 2013;82(10):1677-82. https://doi.org/10.1016/j.ejrad.2013.05.013.
15. World Cancer Research Find International. 2024. Prostate cancer statistics [Internet]. London: WCRF; 2021 [updated 2021; cited 2024 Mar 3]. Available from: https://www.wcrf.org/cancer-trends/prostate-cancer-statistics/.
16. Kimura T, Takahashi H, Okayasu M, Kido M, Inaba H, Kuruma H, et al. Time trends in histological features of latent prostate cancer in Japan. J Urol. 2016;195:1415-20. https://doi.org/10.1016/j.juro.2015.11.068.
17. Chun FKH, Suardi N, Capitanio U, Jeldres C, Ahyai S, Graefen M, et al. Assessment of pathological prostate cancer characteristics in men with favorable biopsy features on predominantly sextant biopsy. Eur Urol. 2009;55(3):617-28. https://doi.org/10.1016/j.eururo.2008.04.099.
18. Beauval JB, Ploussard G, Soulié M, Pfister C, Van Agt S, Vincendeau S, et al. Pathologic findings in radical prostatectomy specimens from patients eligible for active surveillance with highly selective criteria: A multicenter study. Urology. 2012; 80(3):656-60. https://doi.org/10.1016/j.urology.2012.04.051.
19. De Visschere PJL, Naesens L, Libbrecht L, Van Praet C, Lumen N, Fonteyne V, et al. What kind of prostate cancers do we miss on multiparametric magnetic resonance imaging?. Eur Radiol. 2016;26(4):1098-107. https://doi.org/10.1007/s00330-015-3894-x.
20. Joshi S, Tilak MA, Jadhav S. Significance of detection of free/total PSA ratio and other biochemical parameters in patients with BPH, carcinoma prostate and its clinicopathologic correlation. Int J Med Med Res. 2021;7(1):42-50. https://doi.org/10.11603/ijmmr.2413-6077.2021.1.12122.
21. Pezaro C, Woo HH, Davis ID. Prostate cancer: Measuring PSA. Intern Med J. 2014;44(5):433-40. https://doi.org/10.1111/imj.12407.
22. Carlsson SV, Vickers AJ. Screening for prostate cancer. Med Clin North Am. 2020;104:1051-62. https://doi.org/10.1016/j.mcna.2020.08.007.
23. Zhang M, Tang J, Luo Y, Wang Y, Wu M, Memmott BS, et al. Diagnostic performance of multiparametric transrectal ultrasound in localized prostate cancer: A comparative study with magnetic resonance imaging. J Ultrasound Med. 2019;38(7):1823-30. https://doi.org/10.1002/jum.14878.
24. Pavlovich CP, Cornish TC, Mullins JK, Fradin J, Mettee LZ, Connor JT, et al. High-resolution transrectal ultrasound: Pilot study of a novel technique for imaging clinically localized prostate cancer. Urol Oncol. 2014;32(1):e27-e32. https://doi.org/10.1016/j.urolonc.2013.01.006.
25. Correas JM, Halpern EJ, Barr RG, Ghai S, Walz J, Bodard S, et al. Advanced ultrasound in the diagnosis of prostate cancer. World J Urol. 2021;39(3):661-76. https://doi.org/10.1007/s00345-020-03193-0.
26. Drost FJH, Osses DF, Nieboer D, Steyerberg EW, Bangma CH, Roobol MJ, et al. Prostate MRI, with or without MRI-targeted biopsy, and systematic biopsy for detecting prostate cancer. Cochrane Database Syst Rev. 2019;4(4):CD012663. https://doi.org/10.1002/14651858.CD012663.pub2.
27. Borghesi M, Ahmed H, Nam R, Schaeffer E, Schiavina R, Taneja S, et al. Complications after systematic, random, and image-guided prostate biopsy. Eur Urol. 2017;71(3):353-65. https://doi.org/10.1016/j.eururo.2016.08.004.
28. Hambrock T, Hoeks C, Hulsbergen-van de Kaa C, Scheenen

T, Fütterer J, Bouwense S, et al. Prospective assessment of prostate cancer aggressiveness using 3-t diffusion-weighted magnetic resonance imaging-guided biopsies versus a systematic 10-core transrectal ultrasound prostate biopsy cohort. Eur Urol. 2012;61:177-84. https://doi.org/10.1016/j.eururo.2011.08.042.
29. Kobus T, Hambrock T, Hulsbergen-van de Kaa C, Wright AJ, Barentsz JO, Heerschap A, et al. In vivo assessment of prostate cancer aggressiveness using magnetic resonance spectroscopic imaging at 3 t with an endorectal coil. Eur Urol. 2011;60:1074-80. https://doi.org/10.1016/j.eururo.2011.03.002.
30. Wang L, Mazaheri Y, Zhang J, Ishill NM, Kuroiwa K, Hricak H. Assessment of biologic aggressiveness of prostate cancer: Correlation of MR signal intensity with Gleason grade after radical prostatectomy. Radiology. 2008;246:168-76. https://doi.org/10.1148/radiol.2461070057.
31. Schouten MG, van der Leest M, Pokorny M, Hoogenboom M, Barentsz JO, Thompson LC, et al. Why and where do we miss significant prostate cancer with multi-parametric magnetic resonance imaging followed by magnetic resonance-guided and transrectal ultrasound-guided biopsy in biopsy-naïve men? Eur Urol. 2017;71(6):896-903. https://doi.org/10.1016/j.eururo.2016.12.006.
32. Onay A, Ertas G, Vural M, Acar O, Saglicam Y, Coskun B, et al. Evaluation of peripheral zone prostate cancer aggressiveness using the ratio of diffusion tensor imaging measures. Contrast Media Mol Imaging. 2017;2017:5678350. https://doi.org/10.1155/2017/5678350.
33. Li C, Chen M, Li S, Zhao X, Zhang C, Luo X, et al. Detection of prostate cancer in peripheral zone: Comparison of MR diffusion tensor imaging, quantitative dynamic contrast-enhanced MRI, and the two techniques combined at 3.0 T. Acta Radiol. 2014;55(2):239-47. https://doi.org/10.1177/0284185113494978.
34. Kim CK, Jang SM, Park BK. Diffusion tensor imaging of normal prostate at 3 T: Effect of number of diffusion-encoding directions on quantitation and image quality. Br J Radiol. 2012;85(1015):e279-e283. https://doi.org/10.1259/bjr/21316959.
35. Abouelkheir RT, Aboshamia YI, Taman SE. Diagnostic utility of three Tesla diffusion tensor imaging in prostate cancer: Correlation with Gleason score values. Egypt J Radiol Nucl Med. 2022;53(1):207. https://doi.org/10.1186/s43055-022-00892-z.
36. Shenhar C, Degani H, Ber Y, Baniel J, Tamir S, Benjaminov O, et al. Diffusion is directional: Innovative diffusion tensor imaging to improve prostate cancer detection. Diagnostics. 2021;11(3):563. https://doi.org/10.3390/diagnostics11030563.
37. Park SY, Kim CK, Park BK, Ha SY, Kwon GY, Kim B. Diffusion-tensor MRI at 3 T: Differentiation of central gland prostate cancer from benign prostatic hyperplasia. Am J Roentgenol. 2014;202:W254-W262. https://doi.org/10.2214/AJR.13.11015.
38. Gürses B, Kabakci N, Kovanlikaya A, Firat Z, Bayram A, Uluð AM, et al. Diffusion tensor imaging of the normal prostate at 3 Tesla. Eur Radiol. 2008;18(4):716-21. https://doi.org/10.1007/s00330-007-0795-7.
39. Sinha S, Sinha U. In vivo diffusion tensor imaging of the human prostate. Magn Reson Med. 2004;52:530-37. https://doi.org/10.1002/mrm.20190.
40. Hectors SJ, Semaan S, Song C, Lewis S, Haines GK, Tewari A, et al. Advanced diffusion-weighted imaging modeling for prostate cancer characterization: Correlation with quantitative histopathologic tumor tissue composition – A hypothesis-generating study. Radiology. 2018;286:918-28. https://doi.org/10.1148/radiol.2017170904.
41. Ertas G. Detection of high GS risk group prostate tumors by diffusion tensor imaging and logistic regression modelling. Magn Reson Imaging. 2018;50:125-33. https://doi.org/10.1016/j.mri.2018.04.003.
42. Lemberskiy G, Rosenkrantz AB, Veraart J, Taneja SS, Novikov DS, Fieremans E. Time-dependent diffusion in prostate cancer. Invest Radiol. 2017;52(7):405-11. https://doi.org/10.1097/RLI.0000000000000356.
43. Cybulski AJ, Catania M, Brancato S, Cogo N, di Paola V, Pozzi Mucelli R, et al. Added value of MRI tractography of peri-prostatic nerve plexus to conventional T2-WI in detection of extra-capsular extension of prostatic cancer. Radiol Med. 2019;124(10):946-54. https://doi.org/10.1007/s11547-019-01047-3.
44. Uribe CF, Jones EC, Chang SD, Goldenberg SL, Reinsberg SA, Kozlowski P. In vivo 3T and ex vivo 7T diffusion tensor imaging of prostate cancer: Correlation with histology. Magn Reson Imaging. 2015;33(5):577-83. https://doi.org/10.1016/j.mri.2015.02.022.
45. Gürses B, Tasdelen N, Yencilek F, Kılıckesmez NO, Alp T, Firat Z, et al. Diagnostic utility of DTI in prostate cancer. Eur J Radiol. 2011;79:172-6. https://doi.org/10.1016/j.ejrad.2010.01.009.
46. Caporale AS, Nezzo M, Di Trani MG, Maiuro A, Miano R, Bove P, et al. Acquisition parameters influence diffusion metrics effectiveness in probing prostate tumor and age-related microstructure. J Pers Med. 2023;13(5):860. https://doi.org/10.3390/jpm13050860.
47. Manenti G, Carlani M, Mancino S, Colangelo V, Di Roma M, Squillaci E, et al. Diffusion tensor magnetic resonance imaging of prostate cancer. Invest Radiol. 2007;42(6):412-9. https://doi.org/10.1097/01.rli.0000264059.46444.bf.
48. Reischauer C, Wilm BJ, Froehlich JM, Gutzeit A, Prikler L, Gablinger R, et al. High-resolution diffusion tensor imaging of prostate cancer using a reduced FOV technique. Eur J Radiol. 2011;80(2):e34-e41. https://doi.org/10.1016/j.ejrad.2010.06.038.
49. Hnatjuk M, Nesteruk S, Tatarchuk L, Monastyrska N. Morphometric aspects of studying the features of age structural reconstruction of the walls of the prostate arteries. Bull Med Biol Res. 2022;4(1):17-20. https://doi.org/10.11603/bmbr.2706-6290.2022.1.12966.
50. Hnatjuk M, Nesteruk S, Tatarchuk L, Monastyrska N. Morphometric assessment of age-related structural changes in the vessels of the microcirculatory bed of the prostate gland under conditions of ethanol intoxication. Bull Med Biol Res. 2023;5(3):8-15. https://doi.org/10.61751/bmbr.2706-6290.2023.3.8.
51. Mulyadi R, Handoko H, Zairinal RA, Prihartono J. The role of pretherapeutic diffusion-weighted MR imaging derived apparent diffusion coefficient in predicting clinical outcomes in immunocompetent patients with primary CNS lymphoma: A systematic review and meta-analysis. Asian Pac J Cancer Prev. 2022;23(7):2449-57. https://doi.org/10.31557/APJCP.2022.23.7.2449.
52. EL Sayed FM, Nassef EM, Abdelmageed NA, Maqsoud RRA, Abosaif AI. Diffusion-weighted MRI as non-invasive diagnostic tool for rectal cancer aggressiveness and correlation with KI-67 expression in tumor tissue. Asian Pac J Cancer Prev. 2022;23:3387-91. https://doi.org/10.31557/APJCP.2022.23.10.3387.
53. Lamasz A, Barg W, Mlynarz P. Is metabolomics the diagnostic tool for medical diagnostics of cancer? Int J Med Med Res. 2018;4(1):35-40. https://doi.org/10.11603/ijmmr.2413-6077.2018.1.8921.
54. Hirna HA, Maltsev DV, Natrus LV, Rozhko MM, Kostyshyn

ID, Tanasiychuk IS. Study of the immunomodulating influence of preparation alpha/beta-defensins on chemo/radiotherapy of patients with oral and oropharyngeal cancer. Fiziologichnyi Zhurnal. 2021;67(4):86-96. https://doi.org/10.15407/fz67.04.086.
55. Yuin JLP, Shin JTJ, Jing CB, Mun TL, Balasubramaniam MA, Wahid DMI. Retrospective analysis of clinical outcomes of stereotactic body radiation therapy for localized prostate cancer at an Asian cancer specialist centre. Asian Pac J Cancer Prev. 2023;24(2):545-50. https://doi.org/10.31557/APJCP.2023.24.2.545.
56. Kozłowski P, Parfieniuk-Kowerda A, Tarasik A, Januszkiewicz M, Czauż-Andrzejuk A, Łapiński TW, et al. Occurrence and clinical characteristics of hepatocellular carcinoma in the north-eastern Poland. Przegl Epidemiol. 2017;71(3):405-15.
57. Trifonov AV, Gazizov AS, Tapalova AS, Kibardina LK, Appazov NO, Voloshina AD, et al. Synthesis and Anticancer Evaluation of Novel 7-Aza-Coumarine-3-Carboxamides. Int J Mol Sci. 2023;24(12):9927. https://doi.org/10.3390/ijms24129927.